AD-A204 171

(2)

OFFICE OF NAVAL RESEARCH

Contract N00014-82K-0612

Task No. NR 627-838

FILE COPY

TECHNICAL REPORT NO. 30

Ultramicroelectrode Ensembles. Comparison of Experimental and Theoretical Responses and Evaluation of Electroanalytical Detection Limits

by

I. Francis Cheng, Lisa D. Whiteley and Charles R. Martin

Prepared for publication

in

Analytical Chemistry

DTIC
ELECTE
JAN 27 1989
S D
CD

Department of Chemistry
Texas A&M University
College Station, TX 77843

January 11, 1989

Reproduction in whole or in part is permitted for any purpose of the United States Government

*This document has been approved for public release and sale; its distribution is unlimited

*This statement should also appear in Item 10 of Document Control Data - DD Form 1473. Copies of form Available form cognizant contract administrator

UNCLASSIFIED

SECURITY CLASSIFICATION OF THIS PAGE (When Data Entered)

REPORT DOCUMENTATION PAGE		READ DISTRUCTIONS BEFORE COMPLETING FORM
1. REPORT NUMBER: Technical Report # 30	2. GOVT ACCESSION NO.	3. RECIPIENT'S CATALOG NUMBER
4. TITLE (and Subtitle): "Ultramicroelectrode Ensembles. Comparison of Experimental and Theoretical Responses and Evaluation of Electroanalytical Detection Limits"		5. TYPE OF REPORT & PERIOD COVERED: Technical Report
		6. PERFORMING ORG. REPORT NUMBER
7. AUTHOR(s): I. Francis Cheng, Lisa D. Whiteley and Charles R. Martin		8. CONTRACT OR GRANT NUMBER(s): N00014-82K-0612
9. PERFORMING ORGANIZATION NAME AND ADDRESS: Department of Chemistry, Texas A&M University, College Station, TX 77843		10. PROGRAM ELEMENT, PROJECT, TASK AREA & WORK UNIT NUMBERS: NR 627-838
11. CONTROLLING OFFICE NAME AND ADDRESS: Office of Naval Research, 800 North Quincy Street, Arlington, VA 22217		12. REPORT DATE: January 11, 1989
		13. NUMBER OF PAGES
14. MONITORING AGENCY NAME & ADDRESS(if different from Controlling Office)		15. SECURITY CLASS. (of this report): UNCLASSIFIED
		15a. DECLASSIFICATION/DOWNGRADING SCHEDULE

16. DISTRIBUTION STATEMENT (of this Report)

APPROVED FOR PUBLIC DISTRIBUTION, DISTRIBUTION UNLIMITED

17. DISTRIBUTION STATEMENT (of the abstract entered in Block 20, if different from Report)

18. SUPPLEMENTARY NOTES

19. KEY WORDS (Continue on reverse side if necessary and identify by block number)

Ultramicrodisk Electrode, Ensembles; Electrochemical response, characteristics; Electroanalytical detection limits. (organ)

20. ABSTRACT (Continue on reverse side if necessary and identify by block number)

Brief. The ultramicroelectrode ensembles yield responses which are in quantitative agreement with predictions of established electrochemical theory. Furthermore, a one order of magnitude improvement in detection limits (relative to a conventional, macro-sized electrode) is demonstrated.

Abstract. In a recent correspondence, we described a new procedure for preparing ultramicrodisk electrode ensembles; the ultramicrodisks were formed

(continued)

DD FORM 1 JAN 73 1473 EDITION OF 1 NOV 65 IS OBSOLETE

S/N 0102-LF-014-6601

UNCLASSIFIED

SECURITY CLASSIFICATION OF THIS PAGE (When Data Entered)

(1)

(Abstract continued)

by filling the pores of a microporous host membrane with carbon paste. In this paper we present results of quantitative and semi-quantitative analyses of the electrochemical response characteristics of these ultramicroelectrode ensembles; we show that the responses are in agreement with predictions of established electrochemical theory. We also show that one of the ensembles investigated here can yield electroanalytical detection limits which are an order of magnitude lower than detection limits at an equivalent macro-sized (0.331 cm^2) electrode.

Contract N00014-82-K-0612

Ultramicroelectrode Ensembles. Comparison of Experimental and Theoretical Responses and Evaluation of Electroanalytical Detection Limits

I. Francis Cheng, Lisa D. Whiteley and Charles R. Martin*

Department of Chemistry
Texas A&M University
College Station, TX 77843-3255

Accession For
NTIS GRA&I
DTIC TAB
Unannounced
Justification
By
Distribution/
Availability Codes
Dist
A-1

QUALITY INSPECTED 4

Brief. The ultramicroelectrode ensembles yield responses which are in quantitative agreement with predictions of established electrochemical theory. Furthermore a one order of magnitude improvement in detection limits (relative to a conventional, macro-sized electrode) is demonstrated.

Abstract. In a recent correspondence, we described a new procedure for preparing ultramicrodisk electrode ensembles; the ultramicrodisks were formed by filling the pores of a microporous host membrane with carbon paste. In this paper we present results of quantitative and semi-quantitative analyses of the electrochemical response characteristics of these ultramicroelectrode ensembles; we show that the responses are in agreement with predictions of established electrochemical theory. We also show that one of the ensembles investigated here can yield electroanalytical detection limits which are an order of magnitude lower than detection limits at an equivalent macro-sized (0.331 cm^2) electrode.

INTRODUCTION

We have recently described a new method for preparing ensembles of ultramicrodisk electrodes (1-3); the ultramicrodisks are prepared by filling the pores of a microporous host membrane with an electronically conductive material. Thus, the pores in the host membrane act as templates for the elements of the ultramicroelectrode ensemble (1-3). This procedure has been used by us and others to prepare Pt, Au, and carbon paste-based ultramicrodisk ensembles (1-4).

We have conducted quantitative and semi-quantitative analyses of the electrochemical response characteristics of carbon paste-based ensembles prepared using the microporous membrane method. These analyses have shown that the electrochemical response characteristics of these ensembles are in agreement with the predictions of established electrochemical theory. Furthermore, we have shown that these ensembles yield electroanalytical detection limits which are lower than detection limits obtained at analogous macro-sized carbon paste electrodes. We report the results of these and related investigations here.

EXPERIMENTAL SECTION

Reagents. $Fe(bpy)_3(ClO_4)_2$ (G.F. Smith), $K_4Fe(CN)_6$ (Aldrich), H_2SO_4 (Fisher), and K_2SO_4 (Fisher) were used as received. Purified water was obtained by passing house distilled water through a Millipore Milli-Q water purification system. Carbopack C carbon particles (Supelco, 80/100 mesh) and high vacuum grease (Dow Corning) were used to prepare the carbon paste.

Membranes. Microporous membranes were obtained from the Nuclepore Corporation. Table I lists nominal and experimentally-determined parameters for these membranes. Nominal values were provided by Nuclepore.

Experimental pore diameters were obtained by manually measuring pores in high resolution electron micrographs of the membranes. Electron microscopic and electrochemical methods were used to obtain experimental pore densities. The electron microscopic method involved counting the pores in low resolution electron micrographs of the membranes. The electrochemical method will be discussed below. The average (center-to-center) distance between pores (d) was calculated via (5)

$$d = 0.5q^{-1/2} \quad (1)$$

where q is the pore density (pores cm^{-2}).

Electrodes and Instrumentation. Carbon paste was prepared by mixing equal weights of carbon powder and high vacuum grease (3). Macro-sized carbon paste electrodes (area = 0.331 cm^2) were prepared using the conventional procedure (6). Ensembles were prepared by rubbing carbon paste into and through the Nuclepore membranes (3). The carbon paste-impregnated membrane was then applied to the face of a macro-sized carbon paste electrode (3,6). Ensembles were prepared from membranes with measured pore diameters of 13, 8 and 3 μm (Table I); these ensembles are designated 13UME, 8UME, and 3UME.

Nuclepore membrane has a dull and a shiny face; the dull face was applied to the substrate electrode (3). We reported previously that the shiny face results from polishing (3); we have since learned that this is incorrect (7). Nuclepore membranes are prepared from solution-cast polycarbonate film (7). The dull face is the side which had been exposed to the casting surface; the shiny face is the side which had been exposed to air during solvent evaporation (7).

A one compartment electrochemical cell, a Ag/AgCl reference electrode, and a carbon rod counter electrode were employed. Either 0.70 M K_2SO_4 or

0.5 M H_2SO_4 served as the supporting electrolyte. The electrochemical instrumentation has been described previously (2,3). Photomicrographs were obtained using a Bausch and Lomb StereoZoom microscope.

Electrochemical Experiments. Cyclic voltammetry was used to evaluate the response characteristics of the ensembles. Peak currents from high scan rate voltammograms were quantitatively analyzed using theory developed by Osteryoung, et al. (8). Details will be presented in the Results and Discussion Section. These quantitative analyses provided the electrochemical pore densities shown in Table I.

RESULTS AND DISCUSSION

Membrane Characterizations. Table I compares nominal and experimentally-determined pore diameters and densities. Two independent methods were used to determine the experimental densities and the agreement between these methods is quite good (Table I). Table I shows that the experimental densities are significantly less than the nominal values. These data suggest that the nominal densities are erroneously high.

Voltammetric Response Limiting Cases. The voltammetric response at an array or ensemble of ultramicrodisks depends on the scan rate of the experiment. Three limiting cases can be identified (2,3,9,10). The first limiting case occurs at very high scan rates, where the diffusion layers are thin and extend linearly from the individual ensemble elements. A normal, peak-shaped, linear diffusion voltammogram (11) should be observed under these conditions; currents should be proportional to the active element area (2,3). We designate this the "linear active" limiting case.

At lower scan rates, radial diffusion fields develop at the ultramicrodisks. If the distance between the disks is large, the

voltammogram becomes sigmoidal and the limiting current (i_l) is given by

$$i_l = 4nFDCrA_gq \qquad (2)$$

where A_g is the geometric area of the electrode, C is the concentration, D is the diffusion coefficient, r is the disk radius, and q is the disk density. Equation 2 defines the "pure radial" limiting case. Finally, at very low scan rates, the diffusion layers at the ultramicrodisks merge to yield a net linear diffusion field and the voltammogram becomes peak-shaped again. In this "total overlap" limiting case, currents are proportional to the total geometric area of the electrode.

Figure 1 compares low scan rate voltammograms obtained at the ensembles with analogous voltammograms obtained at a macro-sized electrode of equivalent geometric area. The ensemble voltammograms are peaked-shaped and show currents similar in magnitude to the macroelectrode voltammograms. These response characteristics suggest that the total overlap case has been achieved (see quantitative analysis, below). Figure 2 shows the "purest radial diffusion-appearing" waves which could be obtained at each ensemble. Note that the small forward and return peaks indicate that the pure radial case has not been achieved at any of these electrodes.

Finally, Figure 3 shows that the ensemble voltammograms become peak-shaped at very high scan rates. Furthermore, currents at the ensembles are much smaller than currents at a macro-sized electrode of equivalent geometric area. While these are clearly characteristics of the linear active limiting case, further analysis will show that only 13UME and 8UME can achieve this limiting case at experimentally accessible scan rates.

Quantitative Analysis of the High Scan Rate Voltammetric Data. At high scan rates, the diffusion layers at the ultramicrodisks are completely isolated,

and the net response is simply the sum of the responses at the individual disks. Therefore, theory developed for individual ultramicrodisk electrodes can be applied to the ensemble. We show, below, that a value for the element density can be obtained via this analysis.

The parameter p describes the effect of scan rate (ν) and electrode radius (r) on the shape of the ultramicrodisk electrode voltammogram (8).

$$p = (nFr^2\nu/RTD)^{1/2} \quad (3)$$

Osteryoung et al. derived an expression which describes the effect of p on the voltammetric maximum current, I_m (Equation 10 in ref. (8)). The analogous expression for the high scan rate data at the ensemble is

$$I_m = 4nFDCrqA_g\,[0.34\exp(-0.66p) + 0.66 - 0.13\exp(-11/p) + 0.351p] \quad (4)$$

Equation 4 was used to calculate theoretical plots of I_m vs. $\nu^{1/2}$. Typical plots are shown in Figure 4 (solid curves). The curves in Figure 4 were calculated assuming r = 1.5 μm, D = 3.7 x 10^{-6} cm^2 s^{-1} (12), and A_g = 0.331 cm^2. Calculated curves for three different element density values are shown in Figure 4. The experimental voltammetric data for 3UME are also shown in Figure 4 (points).

Figure 4 shows that the experimental data and the calculated data agree beautifully when an element density of 1.18 x 10^6 elements per cm^2 is used in the calculation (middle solid curve). By matching the experimental and calculated curves in this way, an electrochemically-determined value for the element density can be obtained. This analysis was done for all of the ensembles studied here.

The pore densities obtained via this electrochemical analysis are essentially identical to the q values obtained from electron micrographs (Table I). As noted earlier, these data indicate that the nominal pore

densities supplied by Nuclepore are in error. Furthermore, these data show that all of the pores in the Nuclepore membrane yield active ensemble elements. Finally, this analysis proves that these new carbon paste ensembles yield electrochemical responses which are in quantitative agreement with the predictions of established theory (8-10).

The pore density and diameter can be used to calculate the fraction of the geometric area which is electrochemically active (2,3), f_e.

$$f_e = r^2q \qquad (5)$$

In Part I of this series (which dealt with Pt-based ensembles) we compared electrochemically-determined f_e values with f_e's calculated from the known membrane characteristics (2). The electrochemical f_e values were spuriously large. We attributed these excessive f_e values to leakage of the solvent between the Pt elements and the Nuclepore pore walls (2).

Fractional active electrode areas for the carbon paste ensembles are shown in Table I. The f_e values obtained from electron micrographs of the membranes are identical to the electrochemically-determined f_e's. Thus, in contrast to the Pt ensembles (2), solvent does not seep into the ensembles investigated here. Seepage is prevented in the carbon paste ensembles because the vacuum grease acts as a sealant. While this vacuum grease approach works well for aqueous electrochemistry, problems might be encountered if these devices were exposed to organic solvents. We are currently investigating this point.

Semiquantitative Analyses of Voltammetric Data. Semiquantitative evaluations were conducted with the aid of plots of $\log(i_{pa})$ vs. $\log(\nu)$, where i_{pa} is the anodic peak current in an $Fe(bpy)_3^{2+}$ voltammogram. These plots graphically demonstrate the limiting case behavior discussed above and

provide a means for comparing the experimental data with the predictions of electrochemical theory. A log-log format was required because the scan rate region employed extended over six orders of magnitude.

Figure 5A compares plots of $\log(i_{pa})$ vs. $\log(\nu)$ for 3UME with the analogous plot for a macro-sized electrode of equivalent geometric area (points are experimental data; solid curve is the best fit line; ignore, for the moment, the dashed line). As would be expected for a reversible couple, the slope of the macro-sized electrode line is 0.5 (11). At low scan rates, the 3UME curve converges with the macroelectrode line; these data provide quantitative proof that the total overlap case can be achieved at 3UME. While the analogous curve for 8UME (Figure 5B) approaches the macroelectrode line, convergence does not occur. 8UME and 13UME (not shown) do not achieve the total overlap case because the elements in these ensembles are further apart than the elements in 3UME (see Table I).

At higher scan rates, peak currents at the ensembles are smaller than the i_{pa}'s at the macroelectrode (Figure 5). This signals the approach to the pure radial limiting case, where current is independent of scan rate (Equation 2). However, as indicated by the voltammograms in Figure 2, there is no region where pure radial diffusion is achieved (i.e., the slopes of the ensemble curves in Figure 5 never go to zero).

The size and density of the elements in an ultramicroelectrode ensemble determine whether the pure radial case is experimentally accessible. If the density is too high, the transition to the pure radial case will occur at inaccessibly high scan rates. Furthermore, even if isolated diffusion layers can be achieved at an experimentally accessible scan rate, the resulting fields could be predominately linear rather than purely radial

(8). That is, a direct transition from the total overlap case to the linear active case could, in principle, occur.

Nuclepore membranes are used for filtration and thus have relatively high pore densities. Furthermore, the membranes used here contain the largest pores offered by the Nuclepore Corporation. This combination of large pores and high densities, undoubtedly accounts for the inability of these ensembles to show the pure radial limiting case (Figure 5).

While the pure radial case cannot be observed experimentally, Equation 2 can be used to calculate the theoretical radial diffusion limiting current (i_l). These calculated i_l values are shown as the dashed lines in Figure 5. If the pure radial case could be achieved, it would be obtained at scan rates intermediate between the two linear diffusion regimes. In agreement with this prediction, note that the calculated i_l lines intersect the experimental lines in the regions between the two linear response regimes. Furthermore, an inflection is observed in the experimental data near the point at which the calculated i_l line crosses the experimental curve. These data add further evidence that the responses of these ensembles are in agreement with the predictions of established electrochemical theory.

At very high scan rates the $\log(i_{pa})$ vs. $\log(\nu)$ plots for 8UME and 13UME become linear again (see e.g. Figure 5B). Furthermore, the slopes of these high scan rate line segments are 0.5, indicating that diffusion to these ensembles is linear (11). These data provide quantitative proof that the linear active limiting case is achieved at 8UME and 13UME.

Because 3UME contains the smallest elements of the ensembles studied here, the radial contribution to the total current is greatest at 3UME. This suggests that higher scan rates would be required to achieve the linear

active case at 3UME than at 8UME or 13UME. The data in Figure 5A corroborate this conclusion; in contrast to 8UME and 13UME, the slope of the high scan rate line segment for 3UME is substantially less then 0.5, indicating that pure linear diffusion has not been achieved.

Electroanalytical Detection Limits. Electroanalytical detection limits at an ultramicroelectrode ensemble can, in principle, be lower than detection limits at an analogous macro-sized electrode. Lower detection limits are obtained because the ratio of the faradaic to the capacitive currents is higher at the ensemble (2,9,10,13). Both the total overlap and pure radial limiting cases can, in principle, show lower detection limits (2,13).

How much lower will the detection limit at the ensemble be? A quantitative answer to this question can be obtained through a comparison of the faradaic and capacitive currents at the ensemble and at a macro-sized electrode of equivalent geometric area. When the total overlap case is operative, the faradaic currents at the ensemble and the macro-sized electrode are identical (Figure 5A). The capacitive current at the macro-sized electrode ($i_{c,m}$) can be approximated by $i_{c,m} = \nu C_d A_g$, where C_d is the double layer capacitance. The capacitive current at the ensemble ($i_{c,u}$) is given by $i_{c,u} = \nu C_d A_a$, where A_a is the active electrode area (2).

Because A_a will always be less than A_g, $i_{c,u}$ will always be less than $i_{c,m}$. The theoretically expected improvement in detection limit at the ensemble can be calculated by dividing $i_{c,u}$ by $i_{c,m}$; the quotient is just the ratio of the active to geometric areas or the fractional electrode area calculated via Equation 5. Thus, Table I suggests that the 3UME, 8UME and 13UME should yield detection limits which are 0.09, 0.06 and 0.08 times the detection limit at the analogous macro-sized electrode.

Figure 6 compares the voltammogram obtained at 3UME, for a dilute $Fe(CN)_6^{4-}$ solution, with the analogous voltammogram obtained at the macro-sized electrode. The dashed lines in Figure 6 are the experimental background currents obtained at each electrode. In agreement with the above analysis background currents at 3UME are lower, and as a result the signal to background ratio is higher. (The difference in current sensitivities in Figures 6 A and B results because the preponderance of current at the macroelectrode is capacitive.) Figure 7 compares the $Fe(CN)_6^{4-}$ calibration curve obtained at 3UME with the analogous curve for the macro-sized electrode; as anticipated, 3UME shows a lower detection limit.

To obtain a quantitative value for the magnitude of the improvement in detection limit, we define detection limit as that concentration that gives a faradaic signal which is equal to the background current. (Note that since we will ratio the detection limits at the electrodes, other definitions would yield identical results). The detection limits obtained are 44 and 474 nM for 3UME and the macro-sized electrode, respectively. The ratio of these detection limits is 0.09 which is identical to the anticipated ratio (vide supra and Table I).

CONCLUSIONS

We are currently investigating the electrochemical responses of ensembles prepared from membranes which were custom made for us by the Poretics Corporation. The pore diameters and densities were tailored such that these membranes should yield ensembles with detection limits which are as much as three orders of magnitude lower than detection limits at conventional electrodes. We will report the results of these investigations soon.

REFERENCES

1. Martin, C.R. in, Fleischmann, M.; Pons, S.; Rolison, D.R.; Schmidt, P.P. Eds. *Ultramicroelectrodes*; Datatch Systems, Inc: Morgantown, N.C. 1987.
2. Penner, R.M.; Martin, C.R. *Anal. Chem.* 1987, 59, 2625.
3. Cheng, I.F.; Martin, C.R. *Anal. Chem.* 1988, 60, 2163.
4. Wang, J.; Zadeii, J.M. J. Electroanal. Chem. 1988, 249, 339.
5. Scharifker, B.R. *J. Electroanal. Chem.* 1988, 240, 61.
6. Dryhurst, G.; McAllister, D.L. in Laboratory Techniques in Electroanalytical Chemistry; Kissinger, P.T.; Heineman, W.R. Eds.; Marcel Dekker: New York, NY 1984; pp. 294-301.
7. Personal Communication, George Schexnayder, Mobay Corp. Pittsburgh, PA, Sept. 16, 1988 Corp. July, 1988.
8. Aoki, K.; Akimoto, K.; Tokuda, K.; Matsuda, H.; Osteryoung, J. *J. Electroanal. Chem.* 1984, 17, 219.
9. Reller, H.; Kirowa-Eisner, E.; Gileadi, E. *J. Electroanal. Chem. Interfacial Electrochem.* 1984, 161, 247.
10. Cassidy, J.; Ghoroghchian, J.; Sarfarazi, F.; Smith, J.J.; Pons, S. *Electrochim. Acta* 1986, 31, 629.
11. Bard, A.J.; Faulkner, L.R. Electrochemical Methods; John Wiley and Sons, Inc: New York, NY 1980, Chap. 6.
12. Whiteley, L.D. Unpublished results, Texas A&M University, July, 1988.
13. Wehmeyer, K.R.; Deakin, M.R.; Wightman, R.M. *Anal. Chem.* 1985, 57, 1913.

Credit This work was supported by the Office of Naval Research, the Robert A. Welch Foundation, and the Dow Chemical Company.

Table I. Nominal and Experimental Membrane Characteristics

Pore Diameter (μm)		Pore Density (Pores cm^{-2})			Average Distance Between Pores (μm)	f_e[e]	
Nominal[a]	Electron Microscopic[b]	Nominal[a]	Electron Microscopic[b]	Electro-Chemical[c]	Electrochemical[d]	Electron Microscopic[b]	Electrochemical[c]
12	13 ± 2	1×10^5	$6.4(\pm 0.2) \times 10^4$	6.8×10^4	19	0.08 ± 0.03	0.09
8	7.9 ± 0.9	1×10^5	$8.8(\pm 0.5) \times 10^4$	1.2×10^5	14	0.04 ± 0.01	0.06
3	3.0 ± 0.4	2×10^6	$1.36(\pm 0.04) \times 10^6$	1.2×10^6	4.6	0.10 ± 0.02	0.08

[a] Provided by Nuclepore Corp. product literature.

[b] Obtained from electron micrographs of membranes (see text).

[c] Obtained from electrochemical analysis.

[d] Calculated from the electrochemical pore density using Equation 1.

[e] f_e is defined as the sum of the carbon paste element areas

Figure 1 Cyclic voltammograms for 1.08 mM $Fe(bpy)_3^{2+}$ in 0.7 MK_2SO_4. Scan rate = 1 mV s^{-1}. A. Macro-sized electrode. B. 3UME. C. 8UME. D. 13UME. Geometric area for all electrodes = 0.331 cm^2. The current sensitivity is the same for all four voltammograms (see A).

Figure 2 Voltammograms exhibiting the purest sigmoidal shape obtainable at each ensemble. A. 3UME; scan rate = 10 V s^{-1}. B. 8UME; scan rate = 2 V s^{-1}. C. 13UME; scan rate = 0.2 V s^{-1}. Solutions as per Figure 1.

Figure 3 Cyclic voltammograms for 1.08 mM $Fe(bpy)_3^{2+}$ in 0.7 MK_2SO_4. Scan rate = 200 V s^{-1}. A. 3UME. B. 8UME. C. 13UME.

Figure 4 Simulated (solid curves) and experimental (points) plots of anodic peak current vs. square root of scan rate for an ensemble with 3 μm-diameter elements. The element densities (q's) for the simulated plots are 1.4×10^6 (top), 1.18×10^6 (middle), and 1×10^6 (bottom) elements cm^{-2}. See text for details.

Figure 5 Log(anodic peak current) vs. log(scan rate) for cyclic voltammograms of 1.08 mM $Fe(bpy)_3^{2+}$ in 0.7 M K_2SO_4. A. o - Macro-sized carbon paste electrode (area = 0.331 cm^2). ◇ - 3UME data. B. o - Macro-sized carbon paste electrode (area = 0.331 cm^2) . □ - 8UME data. The dashed lines in both A and B are the calculated (Equation 2) pure radial diffusion current lines for the ensembles (see text for details).

Figure 6 Linear sweep voltammograms for 302 nM $Fe(CN)_6^{4-}$ in 0.5 M H_2SO_4. Scan rate = 5 mV s^{-1}. A. 3UME. B. Macro-sized electrode. Geometric area for both electrodes = 0.331 cm^2.

Figure 7 Anodic peak current from $Fe(CN)_6^{4-}$ voltammograms vs. $[Fe(CN)_6^{4-}]$. Scan rate = 5 mV s^{-1}. Electrolyte = 0.5 M H_2SO_4. A. Macro-sized electrode. B. 3UME.

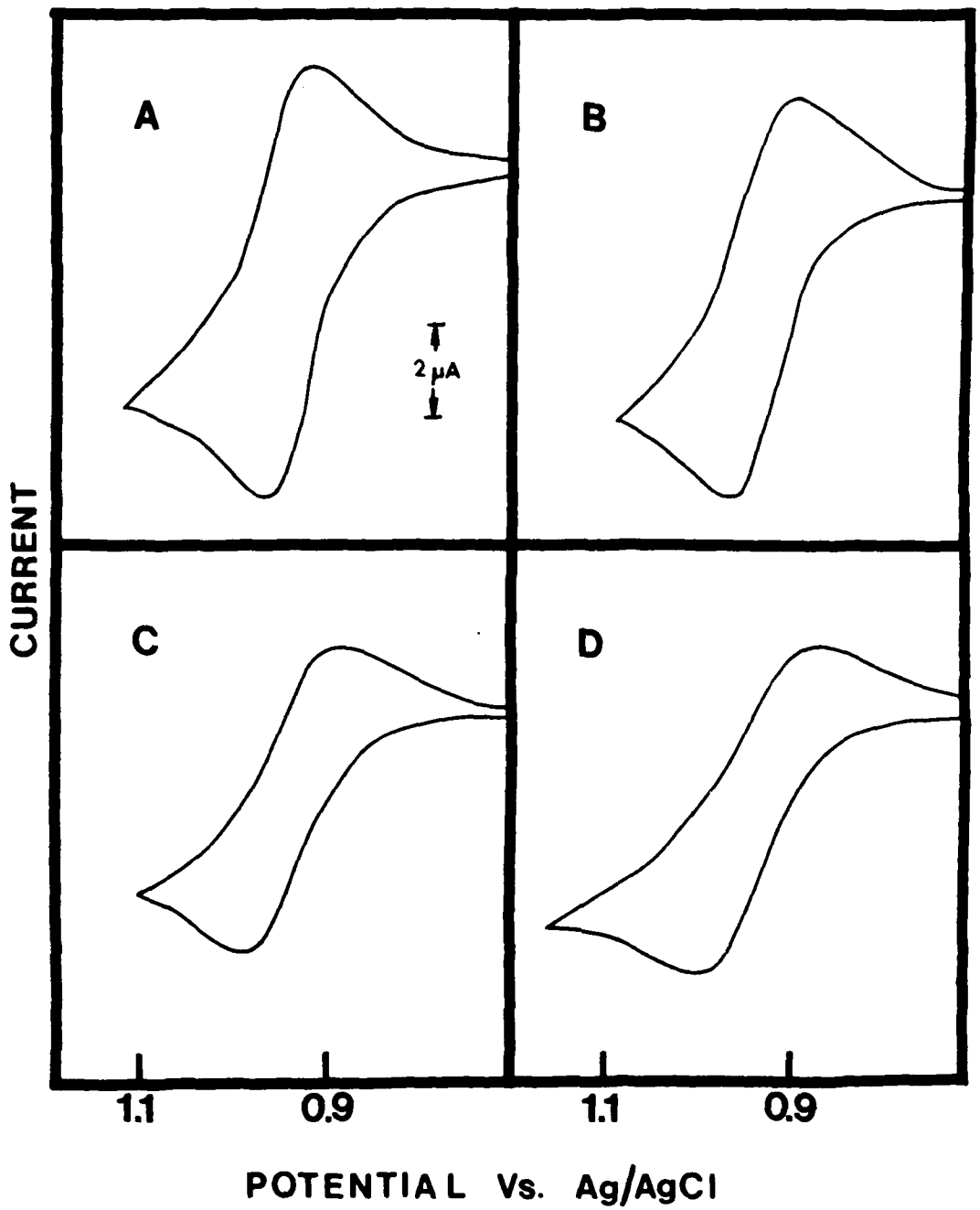
A
B
C
D
2 μA
CURRENT
1.1
0.9
1.1
0.9
POTENTIAL Vs. Ag/AgCl

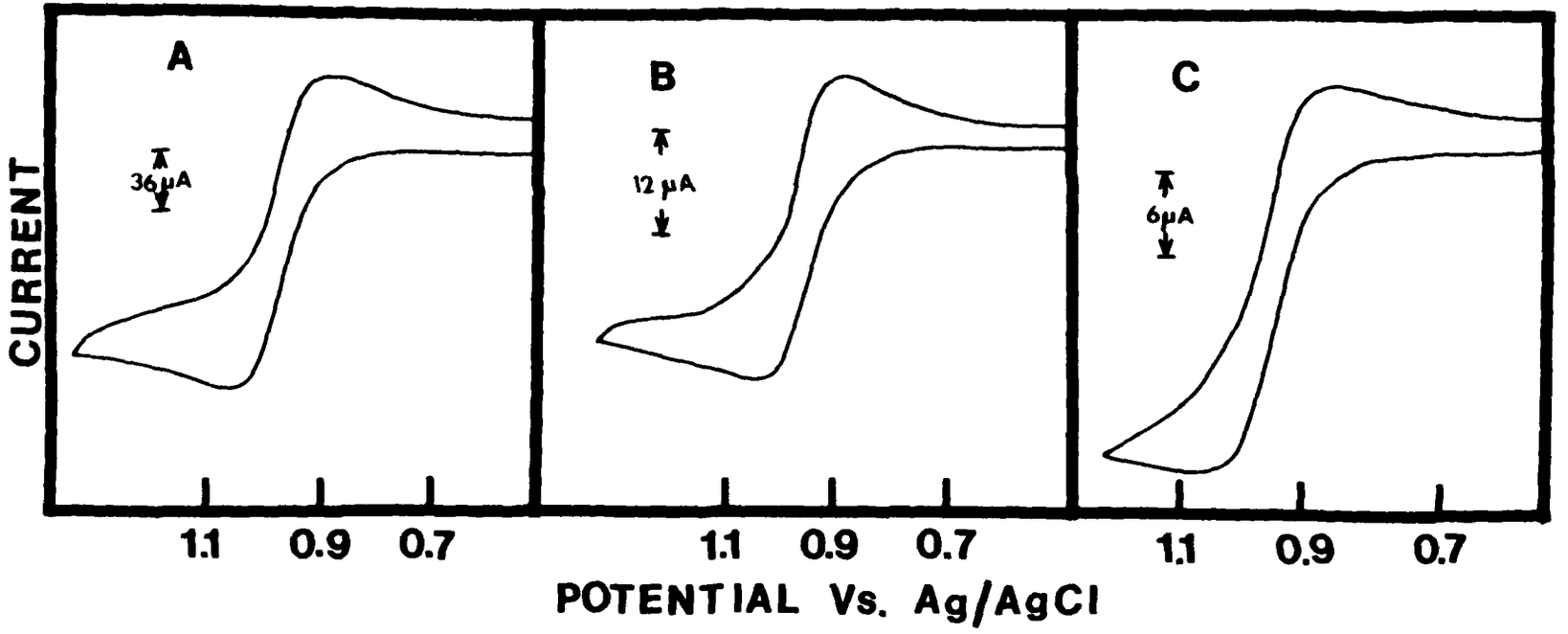
A
36 µA
B
12 µA
C
6µA
CURRENT
1.1
0.9
0.7
1.1
0.9
0.7
1.1
0.9
0.7
POTENTIAL Vs. Ag/AgCl

Fig 2

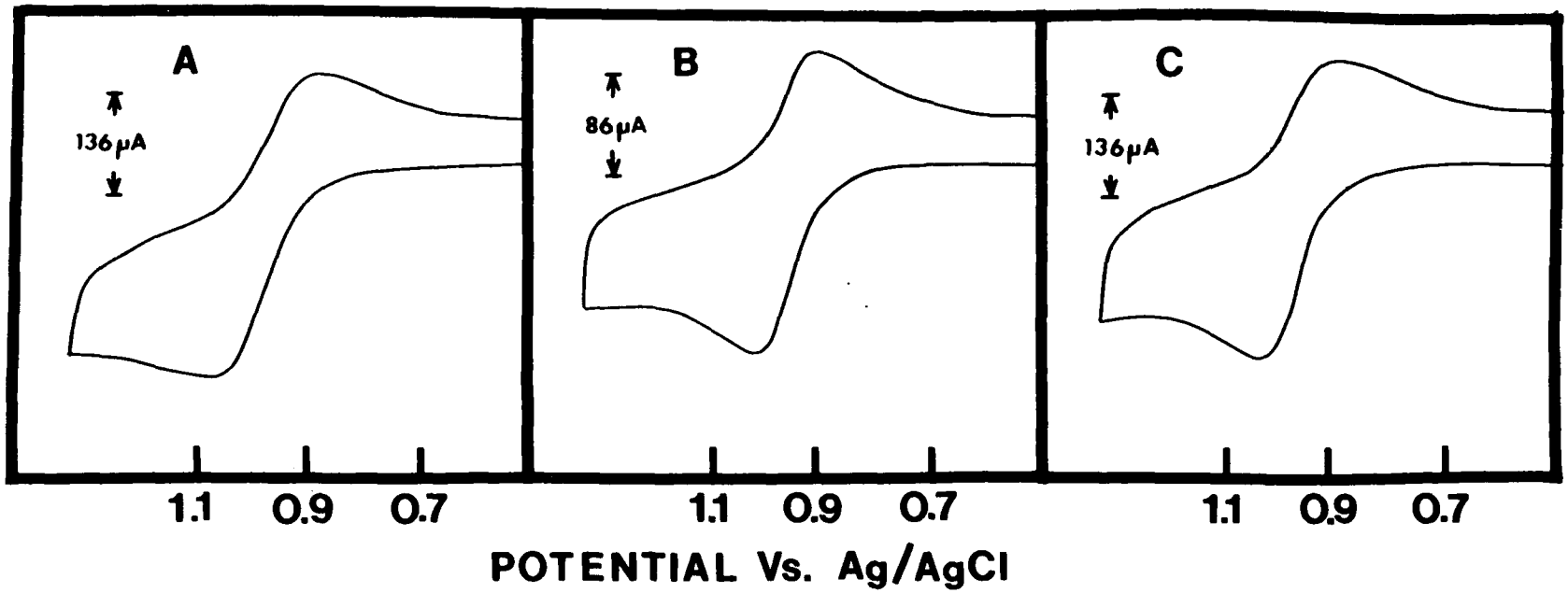
A
136μA
B
86μA
C
136μA
CURRENT
1.1
0.9
0.7
1.1
0.9
0.7
1.1
0.9
0.7
POTENTIAL Vs. Ag/AgCl

Fig 3

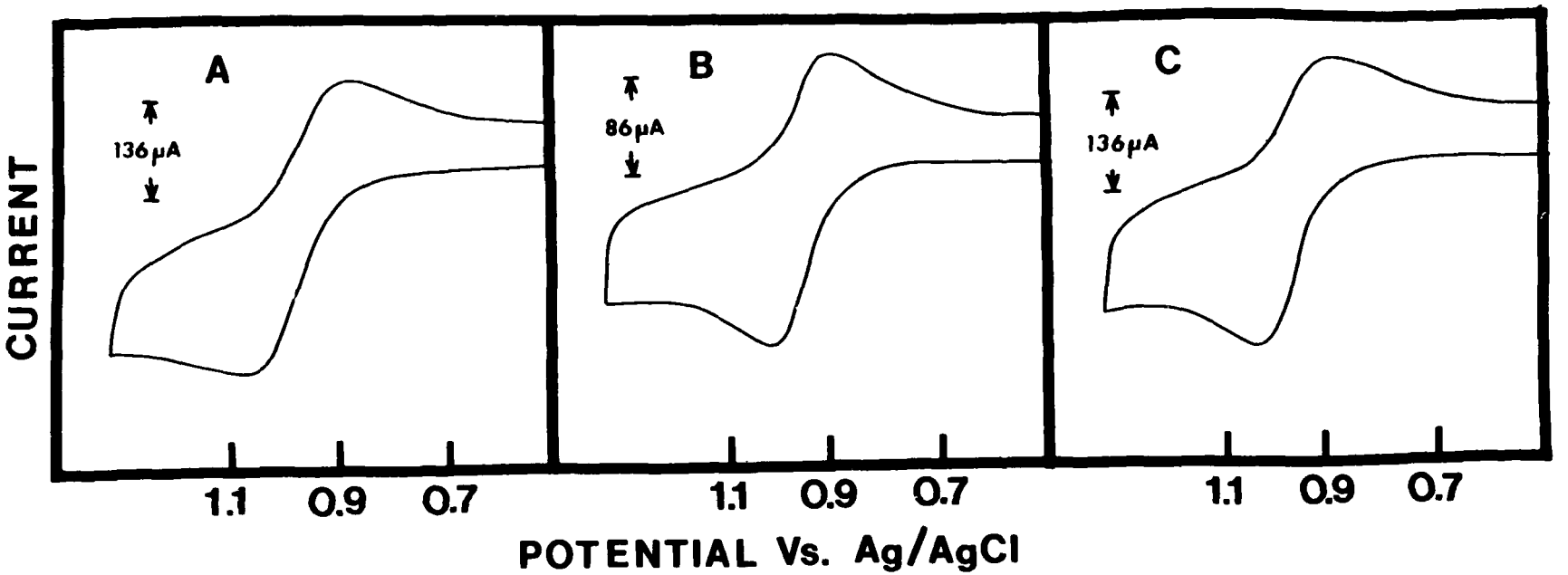
A
136μA
B
86μA
C
136μA
CURRENT
1.1
0.9
0.7
1.1
0.9
0.7
1.1
0.9
0.7
POTENTIAL Vs. Ag/AgCl

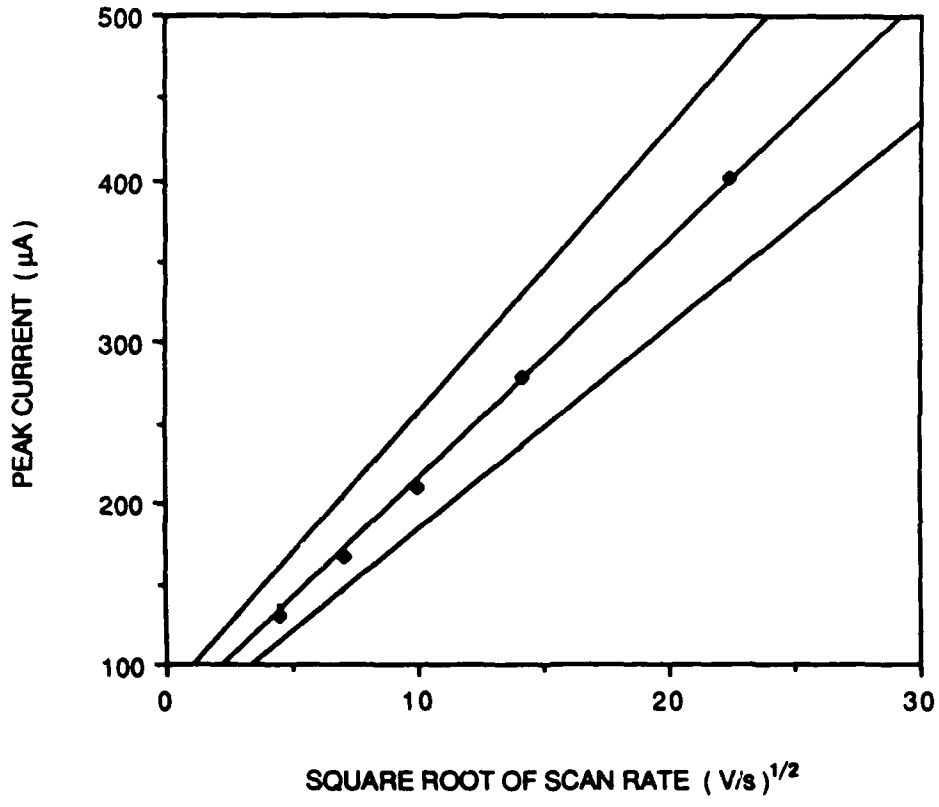
500
400
300
200
100
PEAK CURRENT (μA)
0
10
20
30
SQUARE ROOT OF SCAN RATE (V/s)^1/2

Fig 9

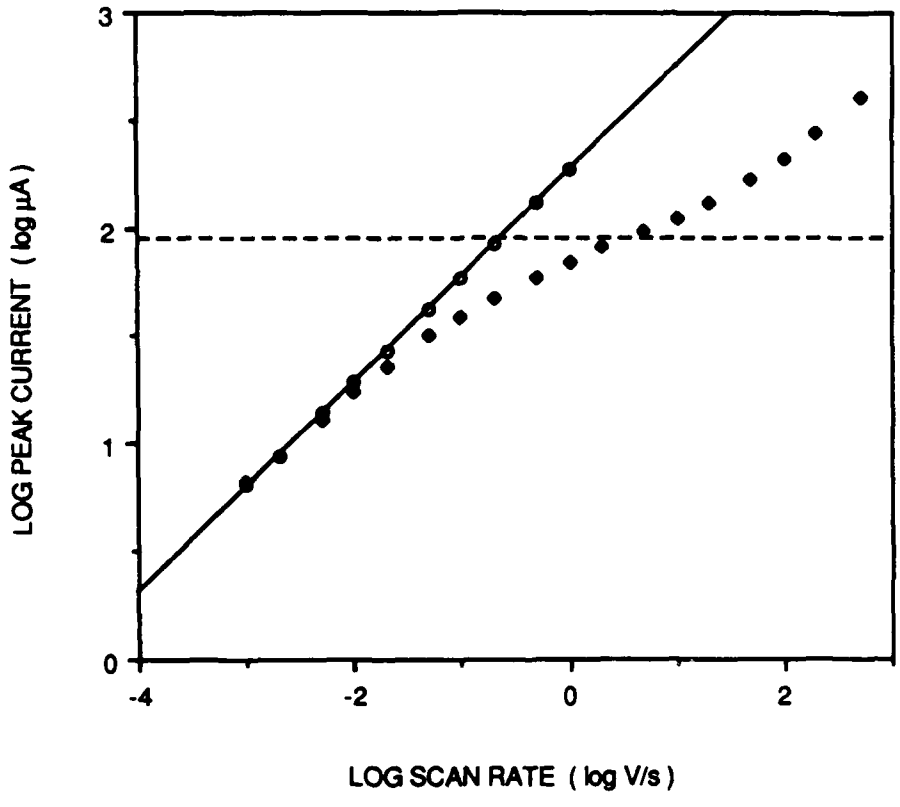

Fig 5A

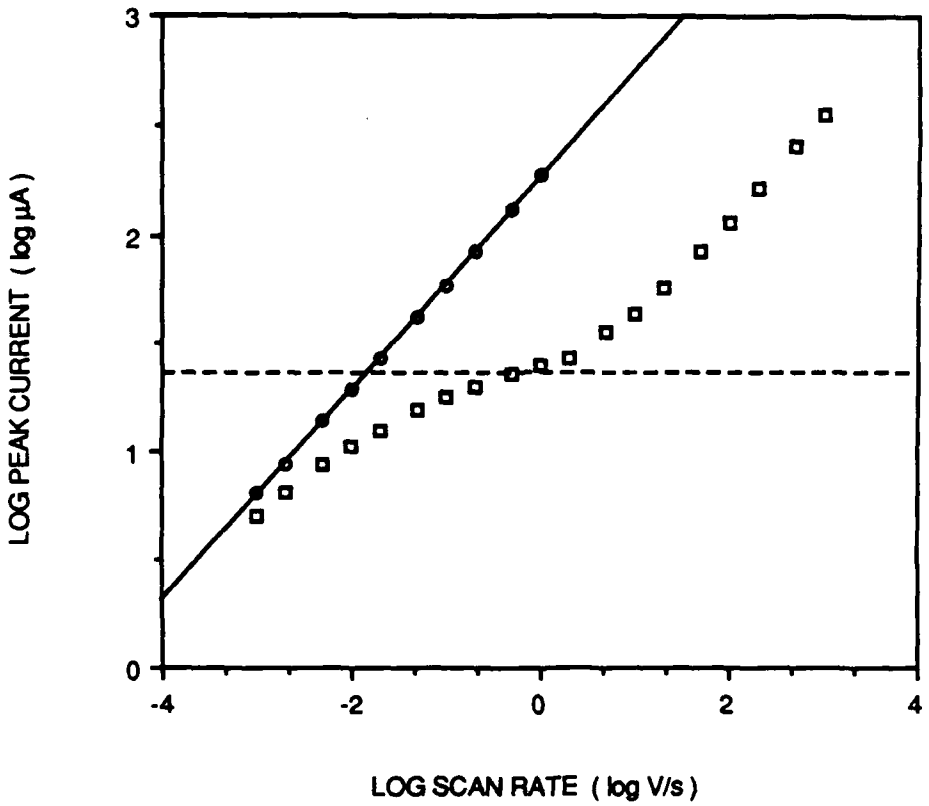

Fig 5B

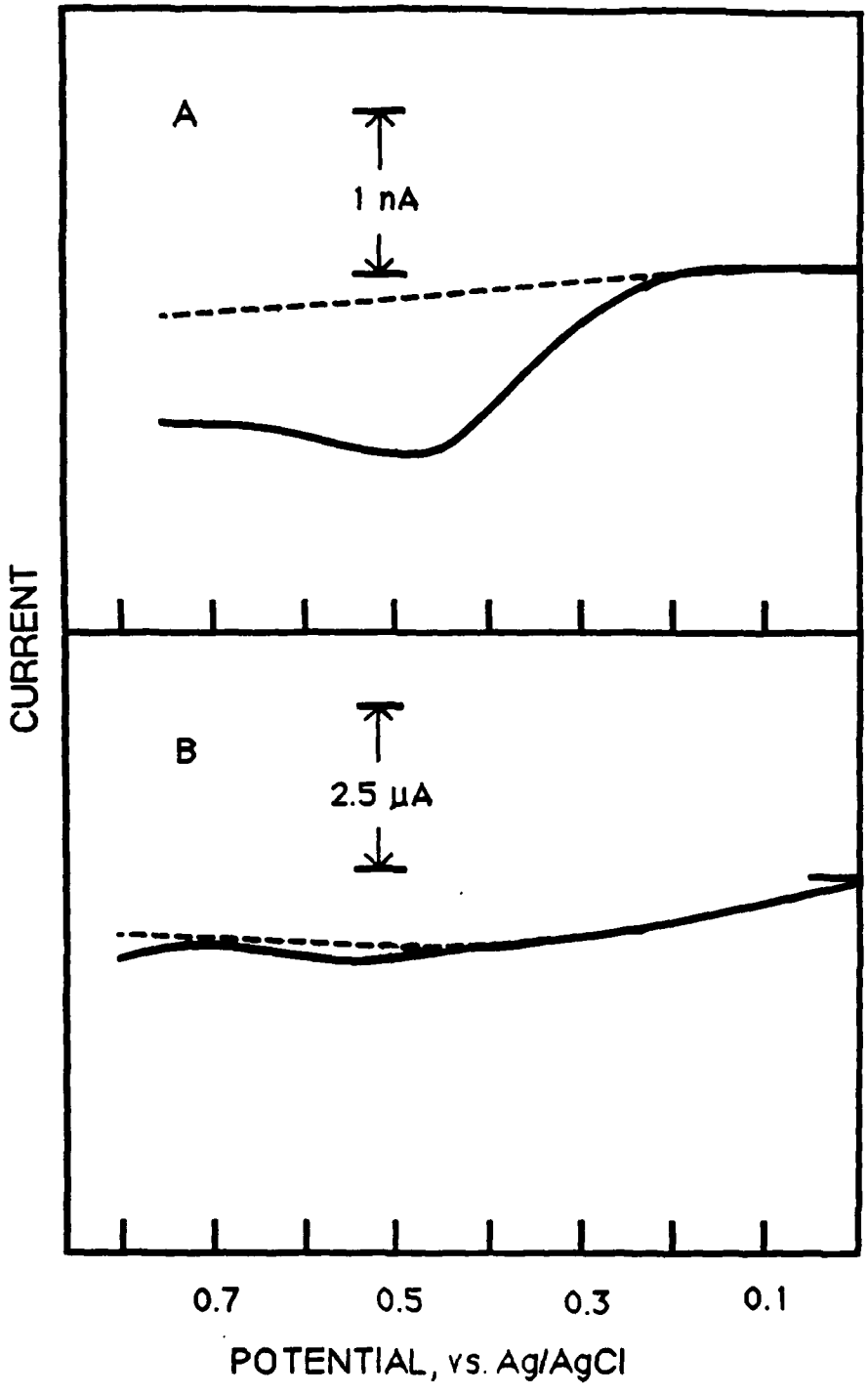

Fig. 6

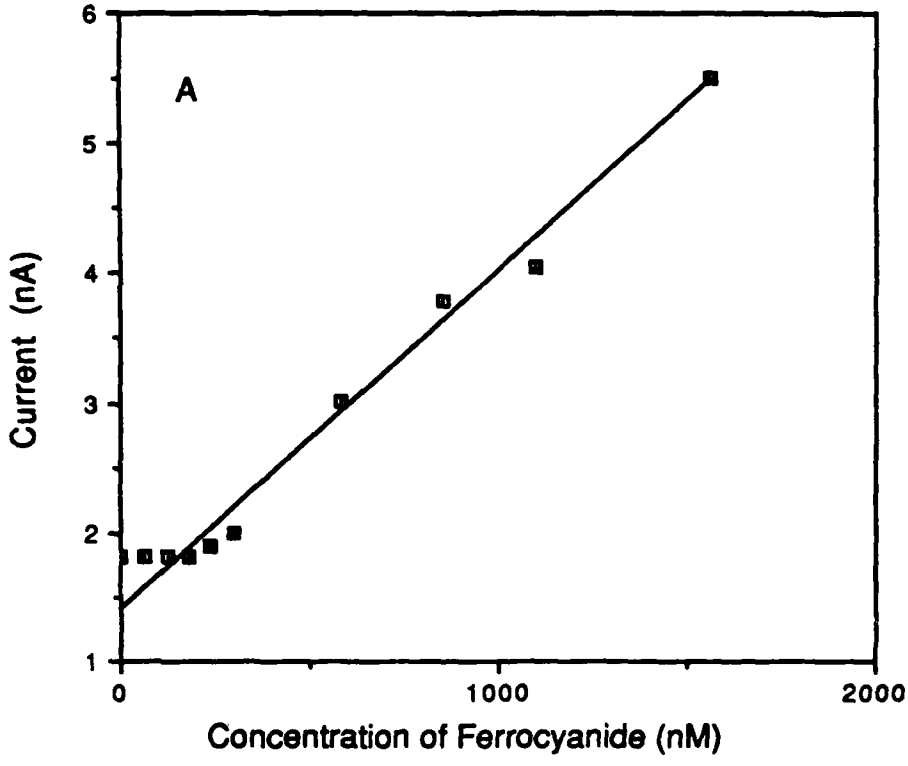
A
Current (nA)
6
5
4
3
2
1
0
1000
2000
Concentration of Ferrocyanide (nM)

Fig 7A

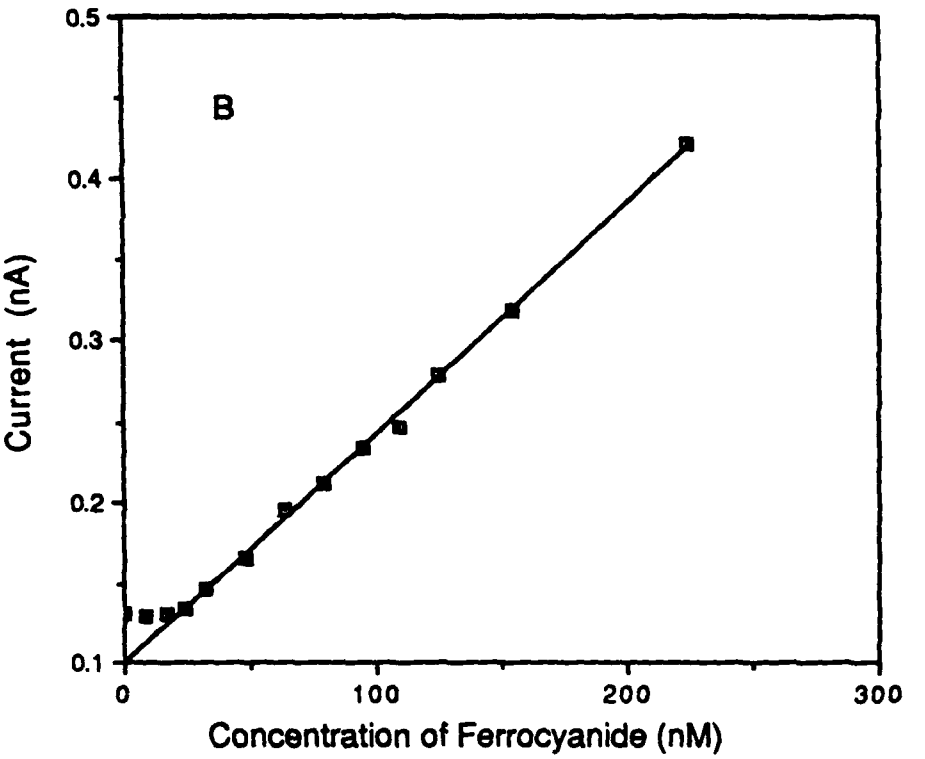
B
0.5
0.4
0.3
0.2
0.1
Current (nA)
0
100
200
300
Concentration of Ferrocyanide (nM)

Fig 7B